Bootstrap for almost cyclostationary processes with jitter effect

Dominique Dehay, Anna Dudek, Mohamed El Badaoui

Bootstrap for almost cyclostationary processes with jitter effect

Dominique Dehay[a], Anna E. Dudek[a,b], Mohamed El Badaoui[c,d]

[a] Institut de Recherche Mathématique de Rennes, UMR CNRS 6625, Université Rennes 2, France.
[b] AGH University of Science and Technology, al. Mickiewicza 30, 30-059 Krakow, Poland.
email: aedudek@agh.edu.pl; tel. +486174405; fax: +486334199.
[c] University of Lyon, UJM-St-Etienne, LASPI, EA3059, F-42023, Saint-Etienne, France.
[d] Safran Tech, Rue des Jeunes Bois – Châteaufort 78772 Magny–les-Hameaux, France.

Abstract

In this paper we consider almost cyclostationary processes with jitter effect. We propose a bootstrap approach based on the Moving Block Bootstrap method to construct pointwise and simultaneous confidence intervals for the Fourier coefficients of the autocovariance function of such processes. In the simulation study we show how our results can be used for second-order frequency detection. We compare behavior of our approach for jitter effects caused by perturbations from two distributions, namely uniform and truncated normal. Finally, we present a real data application of our methodology.

Keywords: almost cyclostationarity, bootstrap, jitter, significance frequency detection.

1 Introduction

In this paper we consider almost cyclostationary (ACS) processes. These are processes that have almost periodic mean and autocovariance function. They are generalizations of cyclostationary (CS) processes for which the mentioned functions are periodic. Let us recall that almost periodic functions were introduced by Besicovitch in [2]. A function $f : \mathcal{R} \to \mathcal{R}$ is called *almost periodic* if for every $\varepsilon > 0$, there exists a number l_ε such that for any interval of length greater than l_ε, there exists a number p_ε in this interval such that

$$\sup_{t\in\mathcal{R}} |f(t + p_\varepsilon) - f(t)| < \varepsilon. \tag{1}$$

Equivalently, the almost periodic functions can be defined as the uniform limits of trigonometric polynomials (see [2]). For more information on ACS and CS processes we refer the reader to [21] and [17].

The analysis of ACS processes is quite challenging. To detect significant frequencies, Fourier expansions of the mean and the autocovariance function are considered. Although, results establishing the estimators of the mentioned Fourier coefficients and their properties are well known (see [16]), in practical applications one needs also a method to obtain the range of possible values of considered parameters. Unfortunately, the asymptotic confidence intervals cannot be constructed because the asymptotic variances of the estimators depend on the unknown parameters. Thus, to compute confidence intervals resampling methods are used. They allow us to approximate the distribution of the statistics of interest. One of the most popular resampling techniques is the bootstrap method. It was introduced by Efron in [13]. The method was at the beginning designed for i.i.d. data, but in the late 80s and beginning of the 90s appeared modifications dedicated for stationary time series (see [18] and [19]). Techniques

for nonstationary case have been developed during the last 10 years. At first appeared results for time domain characteristics of CS and ACS processes ([24], [10], [12]) and later also for the frequency domain parameters ([11], [9], [12], [6]).
In the following we extend applicability of the bootstrap method to the ACS processes with jitter effect, which appears in many signal analysis problems. When acquiring a signal, the jitter of the sampling clock can be voluntary or involuntary. For example, in the case of compressed sensing, it is essential to achieve a random signal acquisition. In practice this operation can be performed by adding a random jitter on the clock signal. In other applications, the jitter can be subjected. This is the case for example of the angular acquisitions vibratory signals from rotating machinery. In this situation, angular sampling is sensitive to hardware imperfections (optical encoder precision, electrical perturbation, etc.). The angular sampled signal quantification step or sampling frequency determination is not identical to the time domain. Angular sampling is also not adapted to study time domain signals like impulse response. Some of these imperfections can be viewed as non-uniform sampling or a random jitter. In these voluntary or involuntary circumstances, it appears appropriate to develop cyclostationary signal analysis tools sampled in the presence of jitter.

The paper is organized as follows. In Section 2 the problem is formulated and the considered assumptions are presented. Moreover, the estimators of the Fourier coefficients are introduced and their asymptotic properties are discussed. Section 3 is dedicated to the bootstrap method. The Moving Block Bootstrap approach adapted to our problem is presented and its consistency for the Fourier coefficients of the autocovariance function is shown. Finally, the construction of the bootstrap pointwise and the simultaneous confidence intervals is provided. Section 4 is devoted to the alternative bootstrap technique that can be used in the considered problem. In Section 5 a simulation study is presented in which the performance of the proposed bootstrap method is verified. Finally, in Section 6 the real data vibratory gear signal is analysed.

2 Problem formulation

Let $X = \{X(t), t \in \mathbb{R}\}$ be a zero-mean real-valued process that is uniformly almost cyclostationary (UACS), i.e. for any $s \in \mathbb{R}$ $\mathrm{E}(X^2(s)) < \infty$ and autocovariance function $B(t,\tau) = \mathrm{Cov}(X_t, X_{t+\tau}) = \mathrm{E}(X(t)X(t+\tau))$ is almost periodic in t uniformly in τ.
In the following we use notation introduced in [7].
The process $X(t)$ is not observed continuously but only in time moments $t_k = kh + U_k, h > 0$. Hence one observes the discrete time process $X_k = \{X(nh + U_k), n \in \mathcal{Z}\}$. Random variables U_k are iid and are independent on X. They can be considered as random errors. In fact we assume that each time moment in which the process is observed is disturbed . This effect is called jitter. In the sequel we assume that $h > 0$ is fixed and small enough to avoid aliasing. In [15] a similar model was considered with U_k being i.i.d. random variables from the standard normal distribution. In this paper we focus on the Fourier analysis of X. Generally, for a fully observed process X, Fourier coefficient of the autocovariance function are of the form

$$a(\lambda,\tau) = \lim_{T\to\infty} \frac{1}{T} \int_0^T \mathrm{E}\left(X(t)X(t+\tau)\right) \exp(-i\lambda s) ds$$

For a continuous time observation of a UAPC process X the estimator

$$\widehat{a}_T(\lambda,\tau) = \frac{1}{T} \int_0^T X(t)X(t+\tau) \exp(-i\lambda t) dt$$

is consistent and asymptotically normal (see e.g. [16], [5]).

To compute the Fourier coefficients of the autocovariance function of X in our case we need to use some approximation. The problem is caused by the fact that we need to know values $X(t)X(t+\tau)$. Since τ is not always a multiple of h, we approximate τ by the nearest multiple of h. Let k_τ be the nearest integer to τ/h. We have

$$\frac{\tau}{h} - \frac{1}{2} < k_\tau < \frac{\tau}{h} + \frac{1}{2}.$$

Finally, $U_{k,\tau} = U_{k+k_\tau} + k_\tau h - \tau$ is a time perturbation for the time moment $kh + \tau$.

We observe a sample $\{X(kh + U_k) : 1 \le k \le n\}$. The estimator of $a(\lambda, \tau)$ is defined as follows

$$\widetilde{a}(\lambda, \tau) = \frac{1}{n} \sum_{k=1}^{n} \widetilde{b}_k(\lambda, \tau),$$

where

$$\widetilde{b}_k(\lambda, \tau) = X(kh + U_k)X((k + k_\tau)h + U_{k+k_\tau}) \exp(-i\lambda kh)$$

and $0 \le k \le n$ and $0 \le k + k_\tau \le n$. Note that for fixed $h > 0$ time series $\widetilde{b}_k(\lambda, \tau)$ is APC. In this form the estimator $\widetilde{a}(\lambda, \tau)$ was defined by Dehay and Monsan (2007) [7]. The authors considered the jitter effect assuming that $h \to 0$ as $n \to \infty$.
In the next subsection we discuss the assumptions that we use to derive our results.

2.1 Assumptions

In the sequel the following conditions are used:

(i) X is sampled at a constant rate greater than the Nyquist rate with time step $h > 0$ (h is small enough to avoid aliasing);

(ii) the random perturbations U_k are i.i.d. from some distribution on $(-h/2, h/2)$;

(iii) set $\Lambda = \{\lambda \in \mathbb{R} : a(\lambda, \tau) \neq 0 \text{ for some } \tau \in \mathbb{R}\}$ is finite;

(iv) $\sup_t \mathrm{E}|X(t)|^{8+2\eta} < \infty$ for some $\eta > 0$;

(v) X has almost periodic fourth moments, i.e. for each $t \in \mathbb{R}$, $\mathrm{E}\{X(t)^4\} < \infty$; the function $(t, \tau_1, \tau_2, \tau_3) \mapsto \mathrm{E}\{X(t)X(t+\tau_1)X(t+\tau_2)X(t+\tau_3)\}$ is almost periodic in t uniformly with respect to τ_1, τ_2, τ_3 varying in $\mathbb{R}$;

(vi) $X(t)$ is α-mixing and $\sum_{k=1}^{\infty} k\alpha_X^{\frac{\eta}{\eta+4}}(k) < \infty$;

Condition (ii) prevents permutation of observations caused by the jitter effect, i.e. we assume that the time moments of the observations are perturbed but the order of the observations is unchanged. Assumption (iii) denotes that for each τ there is a finite number of non-zero coefficients $a(\lambda, \tau)$ or equivalently a finite number of significant frequencies λ. This condition is not necessary but allows us to simplify the presentation of the results. Finally, to obtain the asymptotic normality of $\widetilde{a}(\lambda, \tau)$ mixing condition (vi) is needed. To be precise process X is called α-mixing if $\alpha_X(k) \to 0$ as $k \to \infty$, where

$$\alpha_X(u) = \sup_t \sup_{\substack{A \in \mathcal{F}_X(-\infty, t) \\ B \in \mathcal{F}_X(t+u, \infty)}} |P(A \cap B) - P(A)P(B)|,$$

and $\mathcal{F}_X(-\infty,t)=\sigma\left(\{X(s):s\leq t\}\right)$ and $\mathcal{F}_X(t+u,\infty)=\sigma\left(\{X(s):s\geq t+u\}\right)$ are σ-fields generated by observations from the past and future, respectively. α-mixing is a dependence measure. When $\alpha_X(u)=0$, it means that observations that are u time unites apart are independent. The m-dependent time series are known to be α-mixing. More details and examples can be found in [8].

2.2 Properties of $\widetilde{a}(\lambda,\tau)$

Below we state the asymptotic normality of $\widetilde{a}(\lambda,\tau)$ in the one-dimensional and in the multidimensional case. From now on, any complex number z we treat as the two-dimensional vector of the form $z=(\Re(z),\Im(z))'$. By $\Re(z)$ and $\Im(z)$ we denote the real and the imaginary part of z. Finally symbol $(\cdot)'$ denotes the transpose of a vector.

Theorem 2.1 *Assume that conditions $(i)-(iii)$ and (vi) are fulfilled. Moreover, let $\sup_t \mathrm{E}|X(t)|^{4+\eta}<\infty$ for some $\eta>0$. Then*

$$\sqrt{nh}\left(\widetilde{a}(\lambda,\tau)-\mathrm{E}\left(\widetilde{a}(\lambda,\tau)\right)\right)\xrightarrow{d}N_2\left(0,B(\lambda,\tau)\right),$$

where

$$\begin{aligned}B(\lambda,\tau) &= \frac{1}{2}\int_{\mathbb{R}}\left(b_c(0,\tau,t,t+\tau)S_1(\lambda t)+b_s(0,\tau,t,t+\tau)S_2(\lambda t)\right.\\ &+ \left. b_c(2\lambda,\tau,t,t+\tau)S_3(\lambda t)+b_s(2\lambda,\tau,t,t+\tau)S_4(\lambda t)\right)dt\end{aligned}$$

and

$$\begin{aligned}b_c(\lambda,u,v,w)&=\lim_{T\to\infty}\frac{1}{T}\int_0^T\mathrm{Cov}\left(X(s)X(s+u),X(s+v)X(s+w)\right)\cos(\lambda s)ds,\\ b_s(\lambda,u,v,w)&=\lim_{T\to\infty}\frac{1}{T}\int_0^T\mathrm{Cov}\left(X(s)X(s+u),X(s+v)X(s+w)\right)\sin(\lambda s)ds,\end{aligned}$$

$$\begin{aligned}S_1(\theta)&=\begin{bmatrix}\cos(\theta) & \sin(\theta)\\ -\sin(\theta) & \cos(\theta)\end{bmatrix},\quad S_2(\theta)=\begin{bmatrix}\sin(\theta) & -\cos(\theta)\\ \cos(\theta) & \sin(\theta)\end{bmatrix},\\ S_3(\theta)&=\begin{bmatrix}\cos(\theta) & \sin(\theta)\\ \sin(\theta) & -\cos(\theta)\end{bmatrix},\quad S_4(\theta)=\begin{bmatrix}-\sin(\theta) & \cos(\theta)\\ \cos(\theta) & \sin(\theta)\end{bmatrix}.\end{aligned}$$

The result above is a direct consequence of Theorem 2.6 in [25]. Before we recall the multidimensional version of Theorem 2.1, we introduce some additional notation. By $\boldsymbol{\lambda}$ and $\boldsymbol{\tau}$ we denote r-dimensional vectors of frequencies and shifts of the form

$$\boldsymbol{\lambda}=(\lambda_1,\ldots,\lambda_r)',\quad \boldsymbol{\tau}=(\tau_1,\ldots,\tau_r)'.$$

Additionally,

$$a(\boldsymbol{\lambda},\boldsymbol{\tau})=\left(\Re(a(\lambda_1,\tau_1)),\Im(a(\lambda_1,\tau_1)),\ldots,\Re(a(\lambda_r,\tau_r)),\Im(a(\lambda_r,\tau_r))\right)'$$

and $\widetilde{a}(\boldsymbol{\lambda},\boldsymbol{\tau})$ is its estimator.

Theorem 2.2 *Under assumptions of Theorem 2.1*

$$\sqrt{nh}\left(\widetilde{a}(\boldsymbol{\lambda},\boldsymbol{\tau})-\mathrm{E}\left(\widetilde{a}(\boldsymbol{\lambda},\boldsymbol{\tau})\right)\right)\xrightarrow{d}N_{2r}\left(0,B(\boldsymbol{\lambda},\boldsymbol{\tau})\right),$$

where elements of $B(\boldsymbol{\lambda}, \boldsymbol{\tau})$ *are calculated as follows*

$$\begin{aligned} B(\lambda_i, \lambda_j, \tau_i, \tau_j) &= nh\mathrm{Cov}\left(\widetilde{a}(\lambda_i, \tau_i), \widetilde{a}(\lambda_j, \tau_j)\right) \\ &= \frac{1}{2}\int_{\mathbb{R}} (b_c(\lambda_i - \lambda_j, \tau_i, t, t+\tau_j)S_1(\lambda_j t) + b_s(\lambda_i - \lambda_j, \tau_i, t, t+\tau_j)S_2(\lambda_j t) \\ &+ b_c(\lambda_i + \lambda_j, \tau_i, t, t+\tau_j)S_3(\lambda_j t) + b_s(\lambda_i + \lambda_j, \tau_i, t, t+\tau_j)S_4(\lambda_j t))\, dt \end{aligned}$$

for $i, = 1 \ldots, r$. *The symbols* $b_c(\lambda, u, v, w), b_s(\lambda, u, v, w)$ *and matrices* $S_1(\theta), \ldots, S_4(\theta)$ *are defined in Theorem 2.1.*

One may note that the asymptotic covariance matrix depends on unknown parameters and in practise is almost impossible to estimate. Thus, to calculate confidence intervals resampling methods are used. In the next section we introduce a bootstrap algorithm to construct a family of estimates which will permit us to determine the empirical confidence intervals for $a(\lambda, \tau)$.

3 Bootstrap method

Before we present our bootstrap algorithm, we introduce a decomposition of $\widetilde{a}(\lambda, \tau)$.

$$\widetilde{a}(\lambda, \tau) = \frac{1}{n}\sum_{k=1}^{n} \widetilde{b}_k(\lambda, \tau) = \frac{1}{n}\sum_{k=1}^{n} \ddot{b}_k(\tau)\exp(-i\lambda k h),$$

where

$$\ddot{b}_k(\tau) = X(kh + U_k)X\left((k + k_\tau)h + U_{k+k_\tau}\right).$$

Note that $\ddot{b}_k(\tau)$ is an APC time series.
Let us recall that we observe a sample $(X(h + U_1), X(2h + U_2), \ldots, X(nh + U_n))$. In the following we perform bootstrap on

$$\left(\ddot{b}_1(\tau), \ldots, \ddot{b}_n(\tau)\right), \tag{2}$$

where τ is fixed. Our bootstrap method is based on the Moving Block Bootstrap (MBB) algorithm introduced independently by Künsch (1989) and Liu and Singh (1992). At first we recall the usual MBB algorithm and after we discuss its modification that we used to construct a consistent bootstrap estimator of $a(\lambda, \tau)$.

MBB algorithm
Let $(Y_1, \ldots, Y_n)$ be an observed sample and $B_i = (Y_i, \ldots, Y_{i+b-1}), i = 1, \ldots, n - b + 1$ be a block of observations, which starts with observation Y_i and has length $b, b \in \mathbb{N}$.

1. Choose a block size $b < n$. Then our sample can be divided into l blocks of length b and the remaining part is of length r, i.e. $n = lb + r$, $r = 0, \ldots, b - 1$.

2. From the set $\{B_1, \ldots, B_{n-b+1}\}$ choose randomly with replacement $l + 1$ blocks $B_1^*, \ldots, B_{l+1}^*$. The probability of choosing any block is $1/(n - b + 1)$.

3. Join the selected $l + 1$ blocks $\left(B_1^*, \ldots, B_{l+1}^*\right)$ and take the first n observations to get the bootstrap sample $(Y_1^*, \ldots, Y_n^*)$ of the same length as the original one.

To obtain the bootstrap sample in our case we will not apply the MBB to the sample (2) directly, since we would entirely loose the information about the time indices of selected observations. This information is crucial to construct the bootstrap consistent estimator of $a(\lambda,\tau)$. Thus, we use the MBB to

$$\left(\left(\ddot{b}_1(\tau),1\right),\ldots,\left(\ddot{b}_n(\tau),n\right)\right).$$

The second coordinate in each pair is informing us about the time index of the observation.

BOOTSTRAP ALGORITHM:

1. Choose the block length $b<n$. Then our sample can be divided into l blocks of length b and the remaining part is of length r, i.e. $n=lb+r$, $r=0,\ldots,b-1$.

2. For $t=1,2,\ldots,n-b+1$ let $B_t=\left(\left(\ddot{b}_t(\tau),t\right),\ldots,\left(\ddot{b}_{t+b-1}(\tau),t+b-1\right)\right)$ be a block of the length b. From the set $\{B_1,\ldots,B_{n-b+1}\}$ we choose randomly with replacement $l+1$ blocks $B_1^*,\ldots,B_{l+1}^*$. This means that

$$P^*\left(B_i^*=B_j\right)=\frac{1}{n-b+1}\quad\text{for}\quad i=1,\ldots,l+1,j=1,\ldots,n-b+1,$$

   where P^* denotes the conditional probability given the sample $\{X(kh+U_k):1\le k\le n\}$.

3. Join the selected $l+1$ blocks $\left(B_1^*,\ldots,B_{l+1}^*\right)$ and take the first n observations to get the bootstrap sample $\left(\left(\ddot{b}_1^*(\tau),1^*\right),\ldots,\left(\ddot{b}_n^*(\tau),n^*\right)\right)$ of the same length as the original one.

The idea behind this bootstrap method was used in [6] for the Fourier coefficients of the mean function of the continuous ACS process.

We define the bootstrap estimator of $a(\lambda,\tau)$ as follows

$$\widetilde{a}^*(\lambda,\tau)=\frac{1}{n}\sum_{k=1}^{n}\ddot{b}_k^*(\tau)\exp(-i\lambda k^*h).$$

Note that using the bootstrap only for $\ddot{b}_k(\tau)$, which does not depend on frequency λ, allows us to calculate the value of $\widetilde{a}^*(\lambda,\tau)$ at the same time for many frequencies λ. Bootstraping $\ddot{b}_k(\tau)\exp(-i\lambda kh)$ requires repetition of the algorithm for each frequency. Thus, our approach leads to a substantial reduction of the computational cost.

Below we state consistency of our bootstrap approach.

Theorem 3.1 *Under assumptions $(i)-(vi)$ and if $b\to\infty$ as $n\to\infty$ such that $b=o(n)$, we have that*

$$\rho\Big(\mathcal{L}\left(\sqrt{nh}\left(\widetilde{a}(\lambda,\tau)-a(\lambda,\tau)\right)\right),\mathcal{L}^*\left(\sqrt{nh}\left(\widetilde{a}^*(\lambda,\tau)-\mathrm{E}^*\widetilde{a}^*(\lambda,\tau)\right)\right)\Big)\xrightarrow{p}0.$$

By ρ we denote any distance metricizing weak convergence of probability measures on $\mathbb{R}^2$.

By $\mathcal{L}\left(\sqrt{nh}\left(\widetilde{a}(\lambda,\tau)-a(\lambda,\tau)\right)\right)$ we denote the probability law of $\sqrt{nh}\left(\widetilde{a}(\lambda,\tau)-a(\lambda,\tau)\right)$ and $\mathcal{L}^*\left(\sqrt{nh}\left(\widetilde{a}^*(\lambda,\tau)-\mathrm{E}^*\widetilde{a}^*(\lambda,\tau)\right)\right)$ is its bootstrap counterpart conditionally on the observed sample $\{X(kh+$

$U_k) : 1 \leq k \leq n\}$. Moreover, E^* is the conditional expectation given the sample.
To present the multidimensional version of Theorem 3.1 let us introduce some additional notation. Let $r, \tau \in \mathbb{N}$ be fixed and

$$\boldsymbol{\lambda} = (\lambda_1, \ldots, \lambda_r)',$$

be vector of frequencies. Moreover, let

$$\begin{aligned} \Re a(\boldsymbol{\lambda}, \tau) &= (\Re a(\lambda_1, \tau), \ldots, \Re a(\lambda_r, \tau))', \\ \Im a(\boldsymbol{\lambda}, \tau) &= (\Im a(\lambda_1, \tau), \ldots, \Im a(\lambda_r, \tau))', \end{aligned}$$

and

$$a(\boldsymbol{\lambda}, \tau) = (\Re a(\lambda_1, \tau), \Im a(\lambda_1, \tau), \ldots, \Re a(\lambda_r, \tau), \Im a(\lambda_r, \tau))'.$$

Finally, the estimator of $a(\boldsymbol{\lambda}, \tau)$ and its bootstrap counterpart are denoted respectively by $\widetilde{a}(\boldsymbol{\lambda}, \tau)$ and $\widetilde{a}^*(\boldsymbol{\lambda}, \tau)$. Theorem below states the consistency of our bootstrap method for $a(\boldsymbol{\lambda}, \tau)$.

Theorem 3.2 *Under the assumptions of Theorem 3.1*

$$\rho\left(\mathcal{L}\left\{\sqrt{nh}\left(\widetilde{a}(\boldsymbol{\lambda}, \tau) - a(\boldsymbol{\lambda}, \tau)\right)\right\}, \mathcal{L}^*\left\{\sqrt{nh}\left(\widetilde{a}^*(\boldsymbol{\lambda}, \tau) - \mathrm{E}^*\widetilde{a}^*(\boldsymbol{\lambda}, \tau)\right)\right\}\right) \xrightarrow{p} 0,$$

where ρ is a metric metricizing weak convergence in $\mathbb{R}^{2r}$.

3.1 Bootstrap confidence intervals

Theorem 3.1 allows us to construct bootstrap percentile pointwise confidence intervals for the real and the imaginary part of $a(\lambda, \tau)$. Let us recall that in practice the asymptotic variance is almost impossible to estimate and hence standard asymptotic confidence intervals cannot be obtained. Bootstrap methods are an alternative approach which provide an estimate of the confidence interval estimate for the unknown parameter. Below we discuss the construction of the $(1-\alpha)\%$ bootstrap percentile equal-tailed confidence interval for $\Re a(\lambda, \tau)$. The confidence interval for $\Im a(\lambda, \tau)$ can be got correspondingly.

Bootstrap pointwise confidence intervals

1. Let frequency λ and shift τ be fixed. Repeat B times the bootstrap algorithm described in Section 3 to obtain B replicates of $\widetilde{a}^*(\lambda, \tau)$, i.e. $\widetilde{a}^{*1}(\lambda, \tau), \ldots, \widetilde{a}^{*B}(\lambda, \tau)$.

2. Calculate the mean of the obtained values, i.e.

$$\overline{a}^*(\lambda, \tau) = \frac{1}{B}\sum_{i=1}^{B} \widetilde{a}^{*i}(\lambda, \tau).$$

3. For $i = 1, \ldots, B$ calculate $y_i = \sqrt{nh}\left(\widetilde{a}^{*i}(\lambda, \tau) - \overline{a}^*(\lambda, \tau)\right)$ and sort the obtained values in ascending order to obtain $y_{(1)}, \ldots, y_{(B)}$.

4. Let $k_1 = \lceil B\alpha/2 \rceil$ and $k_2 = \lfloor B(1-\alpha/2) \rfloor$. By $\lceil x \rceil$ and $\lfloor x \rfloor$ we denote the ceiling and the floor of the real number x. The $(1-\alpha)\%$ bootstrap percentile equal-tailed confidence interval for $\Re a(\lambda, \tau)$ is of the form

$$\left(\Re\widetilde{a}(\lambda, \tau) - \frac{y_{(k_2)}}{\sqrt{nh}}, \Re\widetilde{a}(\lambda, \tau) - \frac{y_{(k_1)}}{\sqrt{nh}}\right).$$

In practice for each τ many frequencies are considered. Thus, the simultaneous confidence intervals are of great importance. They are frequently met in real data applications. To obtain them the consistency of the bootstrap approach for smooth functions of $a(\boldsymbol{\lambda}, \tau)$ needs to be shown. This result is a direct consequence of Theorem 3.2 and the continuous mapping theorem.
Below we present the construction of the $(1-\alpha)\%$ bootstrap percentile equal-tailed simultaneous confidence intervals for $\Re a(\lambda_1, \tau), \ldots, \Re a(\lambda_r, \tau)$.

Bootstrap simultaneous confidence intervals

1. Let frequencies $\lambda_1, \ldots, \lambda_r$ and shift τ be fixed. Repeat B times the bootstrap algorithm described in Section 3 to obtain B replicates $\widetilde{a}^{*i}(\boldsymbol{\lambda}, \tau) = (\widetilde{a}^{*i}(\lambda_1, \tau), \ldots, \widetilde{a}^{*i}(\lambda_r, \tau)), i = 1, \ldots, B$.
2. For $j = 1, \ldots, r$ calculate the means of the obtained values, i.e.
$$\overline{a}^*(\lambda_j, \tau) = \frac{1}{B} \sum_{i=1}^{B} \widetilde{a}^{*i}(\lambda_j, \tau).$$
3. For $i = 1, \ldots, B$ calculate
$$K_{max,i} = \sqrt{nh} \max_j \Re \left(\widetilde{a}^{*i}(\lambda_j, \tau) - \overline{a}^*(\lambda_j, \tau) \right),$$
$$K_{min,i} = \sqrt{nh} \min_j \Re \left(\widetilde{a}^{*i}(\lambda_j, \tau) - \overline{a}^*(\lambda_j, \tau) \right).$$
4. Sort the obtained values in ascending order to obtain $K_{max,(1)}, \ldots, K_{max,(B)}$ and $K_{min,(1)}, \ldots, K_{min,(B)}$.
5. Let $k_1 = \lceil B\alpha/2 \rceil$ and $k_2 = \lfloor B(1-\alpha/2) \rfloor$. The $(1-\alpha)\%$ bootstrap percentile equal-tailed simultaneous confidence intervals for $\Re a(\lambda_1, \tau), \ldots, \Re a(\lambda_r, \tau)$ are of the form
$$\left(\Re\widetilde{a}_n(\lambda_j, \tau) - \frac{K_{max,(k_2)}}{\sqrt{nh}}, \Re\widetilde{a}_n(\lambda_j, \tau) - \frac{K_{min,(k_1)}}{\sqrt{nh}} \right)$$
for $j = 1, \ldots, r$, $\lambda_1, \ldots, \lambda_r \in \mathbb{R}$ and $\tau \in \mathbb{R}$. The confidence intervals for the imaginary case are defined correspondingly.

4 Alternative bootstrap approach

In this section we present a modification of the bootstrap approach presented in Section 3, which allows us to reduce bias of our bootstrap estimator for finite n. We use the idea introduced by Politis and Romano (1992). The usual MBB is using $n-b+1$ blocks of the length b. The observations whose indices are between b and $n-b$ are present in b different blocks, while the observations from the beginning and the end of the sample appear less frequently. For example the first observation is only in the block B_1. Politis and Romano showed that this leads to an increase of the bias of the estimator. To reduce it they proposed to treat the data as wrapped on the circle. Then each observation is present in the same number of blocks. Below we discuss how to apply this idea in our setting.

Let us recall that we apply bootstrap to the sample
$$\left(\left(\ddot{b}_1(\tau), 1 \right), \ldots, \left(\ddot{b}_n(\tau), n \right) \right).$$

By $B_i, i = 1, \ldots, n$ we denote a block of observations that starts with observation $\left(\ddot{b}_i(\tau), i\right)$ and has length b. Note that for $i = 1, \ldots, n-b+1$ we consider exactly the same blocks as defined in Section 3. For $i = n-b+2, \ldots, n$ block B_i is created by joining the observations from the end and the beginning of the sample to get a block of the required length. To be precise

$$B_i = \left(\left(\ddot{b}_i(\tau), i\right), \ldots, \left(\ddot{b}_n(\tau), n\right), \left(\ddot{b}_1(\tau), 1\right), \ldots, \left(\ddot{b}_{b-n+i-1}(\tau), b-n+i-1\right)\right) \quad \text{for} \quad i = n-b+2, \ldots, n.$$

Now each observation appears exactly in the same number of blocks. Below we present the circular version of the bootstrap algorithm presented in Section 3.

Circular bootstrap approach

1. Choose the block length $b < n$. Then our sample can be split into l blocks of length b and the remaining part of length $r < b$, i.e. $n = lb + r$, $r = 0, \ldots, b-1$.
2. From the set $\{B_1, \ldots, B_n\}$ choose randomly with replacement $l+1$ blocks $B_1^*, \ldots, B_{l+1}^*$. The probability of choosing any block is equal to $1/n$.
3. Join the selected $l+1$ blocks $\left(B_1^*, \ldots, B_{l+1}^*\right)$ and take the first n observations to get the bootstrap sample $\left(\left(\ddot{b}_1^*(\tau), 1^*\right), \ldots, \left(\ddot{b}_n^*(\tau), n^*\right)\right)$ of the same length as the original one.

The bootstrap estimator $\widetilde{a}^*(\lambda, \tau)$ and its multidimensional version $\widetilde{a}^*(\boldsymbol{\lambda}, \tau)$ remain unchanged (see definitions in Section 3) except that they are constructed by random selections from the set of n blocks.
As we mentioned above Politis and Romano proposed a circular bootstrap idea to reduce the bias of their estimator. The authors considered stationary time series. Below we investigate if the proposed modification is bringing similar effects in our nonstationary case. Let $n = lb$, i.e. the sample size can be split into l disjoint blocks of the length b. We have that

$$\begin{aligned}
&\mathrm{E}^*\left(\widetilde{a}^*(\lambda, \tau)\right) = \mathrm{E}^*\left(\frac{1}{n}\sum_{k=1}^{n} \ddot{b}_k^*(\tau)\exp(-i\lambda k^* h)\right) \\
&= \frac{1}{n}\mathrm{E}^*\left(\sum_{k=1}^{b} \ddot{b}_k^*(\tau)\exp(-i\lambda k^* h) + \sum_{k=b+1}^{2b} \ddot{b}_k^*(\tau)\exp(-i\lambda k^* h) + \cdots + \sum_{k=(l-1)b+1}^{lb} \ddot{b}_k^*(\tau)\exp(-i\lambda k^* h)\right) \\
&= \frac{1}{n}\sum_{j=1}^{l} \mathrm{E}^*\left(\sum_{k=(j-1)b+1}^{jb} \ddot{b}_k^*(\tau)\exp(-i\lambda k^* h)\right) \\
&= \frac{1}{n}\sum_{j=1}^{l}\frac{1}{n}\sum_{s=1}^{n}\left(\sum_{k=s}^{s+b-1} \ddot{b}_k(\tau)\exp(-i\lambda k h)\right) = \widetilde{a}(\lambda, \tau).
\end{aligned}$$

Note that the sum $\left(\sum_{k=s}^{s+b-1} \ddot{b}_k(\tau)\exp(-i\lambda k h)\right)$ is based on observations belonging to the block B_s. Each time when time index $k > n$ we take $k-n$ instead. For the sake of simplicity we decided not to introduce any additional notation to indicate this fact.
We showed that $\mathrm{E}^*\left(\widetilde{a}^*(\lambda, \tau)\right) = \widetilde{a}(\lambda, \tau)$, which means that $\widetilde{a}^*(\lambda, \tau)$ is the unbiased estimator of $\widetilde{a}(\lambda, \tau)$. This property does not hold if the non-circular bootstrap algorithm is used. If the bootstrap sample

$\left(\left(\ddot{b}_1^*(\tau), 1^*\right), \ldots, \left(\ddot{b}_n^*(\tau), n^*\right)\right)$ is obtained using the standard approach described in Section 3, we get

$$\begin{aligned}
\mathrm{E}^*\left(\widetilde{a}^*(\lambda,\tau)\right) &= \frac{1}{n}\sum_{j=1}^{l}\mathrm{E}^*\left(\sum_{k=(j-1)b+1}^{jb}\ddot{b}_k^*(\tau)\exp(-i\lambda k^* h)\right) \\
&= \frac{1}{n}\sum_{j=1}^{l}\frac{1}{n-b+1}\sum_{s=1}^{n-b+1}\left(\sum_{k=s}^{s+b-1}\ddot{b}_k(\tau)\exp(-i\lambda k h)\right) \\
&= \frac{1}{n-b+1}\left(n\widetilde{a}(\lambda,\tau) - \frac{1}{b}\sum_{j=1}^{b-1}(b-j)\left(\ddot{b}_j(\tau)\exp(-i\lambda j h) + \ddot{b}_{n-j+1}(\tau)\exp(-i\lambda(n-j+1)h)\right)\right)
\end{aligned}$$

and hence $\widetilde{a}^*(\lambda,\tau)$ is biased.
Below we present consistency results for the circular bootstrap approach.

Theorem 4.1 *Under assumptions of Theorem 3.1*

$$\rho\Big(\mathcal{L}\left(\sqrt{nh}\left(\widetilde{a}(\lambda,\tau) - a(\lambda,\tau)\right)\right), \mathcal{L}^*\left(\sqrt{nh}\left(\widetilde{a}^*(\lambda,\tau) - \widetilde{a}(\lambda,\tau)\right)\right)\Big) \xrightarrow{p} 0.$$

Theorem 4.2 *Under the assumptions of Theorem 3.2*

$$\rho\left(\mathcal{L}\left\{\sqrt{nh}\left(\widetilde{a}\left(\boldsymbol{\lambda},\tau\right) - a\left(\boldsymbol{\lambda},\tau\right)\right)\right\}, \mathcal{L}^*\left\{\sqrt{nh}\left(\widetilde{a}^*\left(\boldsymbol{\lambda},\tau\right) - \widetilde{a}\left(\boldsymbol{\lambda},\tau\right)\right)\right\}\right) \xrightarrow{p} 0.$$

Finally, following the reasoning presented in Section 3.1 one may construct the pointwise and the simultaneous confidence intervals for Fourier coefficients using the circular version of our bootstrap approach.

5 Simulation study

In the following we investigate how procedures proposed by us work in practise. For that purpose we consider a signal

$$X(t) = a(t)\cos(2\pi t/10) + b(t),$$

where $a(t)$ is a stationary zero-mean Gaussian processes with standard deviation equal to 0.1 and $b(t)$ is a correlated additive Gaussian noise of the form

$$b(t) = 0.5b(t-1) + 0.25b(t-2) + \epsilon(t),$$

where $\epsilon(t)$ are iid r.v. from the normal distribution with mean equal to 0 and standard deviation equal to 0.05.
The set of the second order cyclic frequencies is of the form

$$\Lambda = \{-0.4\pi, 0, 0.4\pi\}.$$

In each period of length 10 we collect 100 observations. We assume that we observe 100 of periods and hence the length of the sample is $n = 10000$ observations. To detect significant frequencies we construct 95% bootstrap pointwise and simultaneous confidence intervals (see Section 3.1) for $Re\left(a(\lambda,0)\right)$ and $Im\left(a(\lambda,0)\right)$. Due to the symmetry of the cyclic spectrum, we restrict our study to $\lambda \in \{0Hz, 0.01Hz, \ldots, 0.5Hz\}$, using the circular version of our bootstrap approach (see Section 4). We

take two block lengths $b \in \{20, 100\}$, which are equal approximately to $\sqrt[3]{n}$ and $\sqrt{n}$. The number of bootstrap samples $B = 500$. Moreover, we consider two types of random perturbations. In the first case U_i are iid r.v. from the uniform distribution on $(-h/2, h/2)$, while in the second one U_i are iid from the truncated normal distribution (mean and standard deviation respectively equal to 0 and 0.01) i.e., distribution restricted to the interval $(-h/2, h/2)$.
The obtained results are presented in Figures 1-2 (uniform distribution case) and 3-4 (truncated normal distribution case). Independently on the considered distribution and the chosen block length using simultaneous confidence intervals we always detect two frequencies i.e., 0 Hz and 0.2 Hz, which are the true frequencies. The pointwise confidence intervals are provide the same results only for $b = 20$. For $b = 100$ we detect some additional frequencies. These are 0.41, 0.45, 0.49 (uniform distribution case) and 0.47, 0.49, 0.5 (truncated normal distribution case). The simultaneous confidence intervals proposed by us are less sensitive to the block length choice and seem to be a convenient tool for frequency detection.

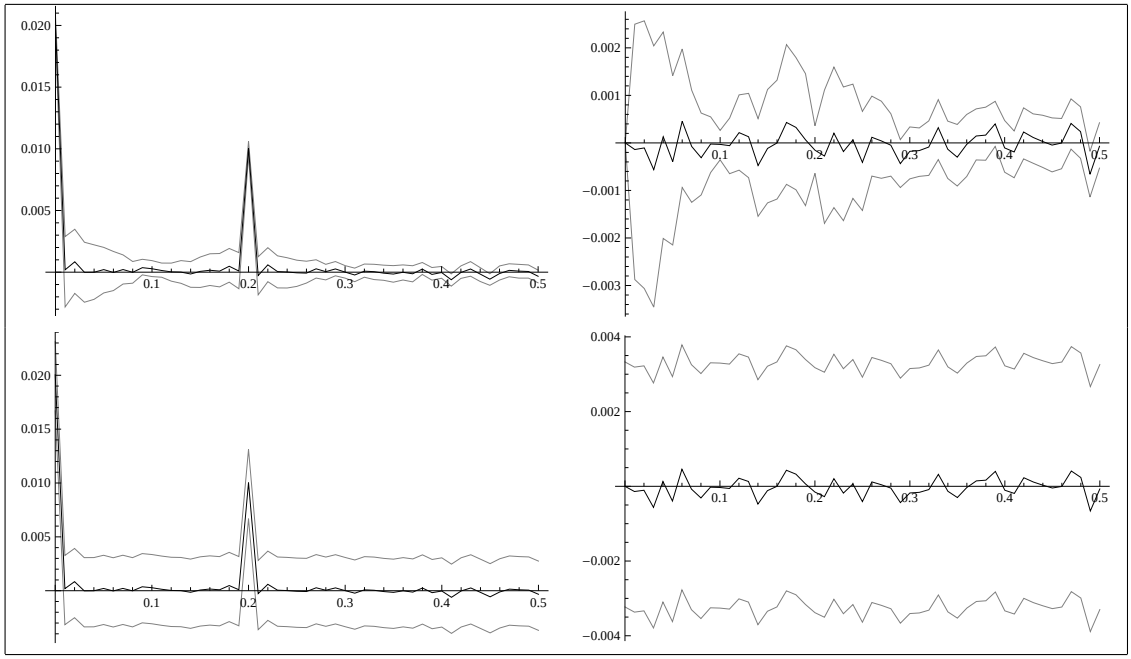

Figure 1: Results for uniform distribution. Grey color: Pointwise (first row) and simultaneous (second row) confidence intervals for $Re\,(a(\lambda, 0))$ (left column) and $Im\,(a(\lambda, 0))$ (right column), $\lambda \in \{0Hz, 0.01Hz, \ldots, 0.5Hz\}$ and $b = 100$. Black color: estimators of $Re\,(a(\lambda, 0))$ and $Im\,(a(\lambda, 0))$. Nominal coverage probability is 95%.

6 Analysis of vibratory gear signals

6.1 Fault detection of a gear system by spectral analysis

Spectral analysis is a natural tool for the processing of signals in mechanics. In general, the vibration signal taken from a rotating machine is a composition that responds to any excitation force. The aim of the spectral analysis is to be able to dissociate and identify of the vibratory sources according to the kinematic characteristics of the various constituent elements and their speed of rotation (or their frequency of movement).

The vibrations resulting from a single stage reduction (Figure 5) are mainly due to the deviation of the position of the wheels with respect to a perfect rotational movement. A number of meshing signal

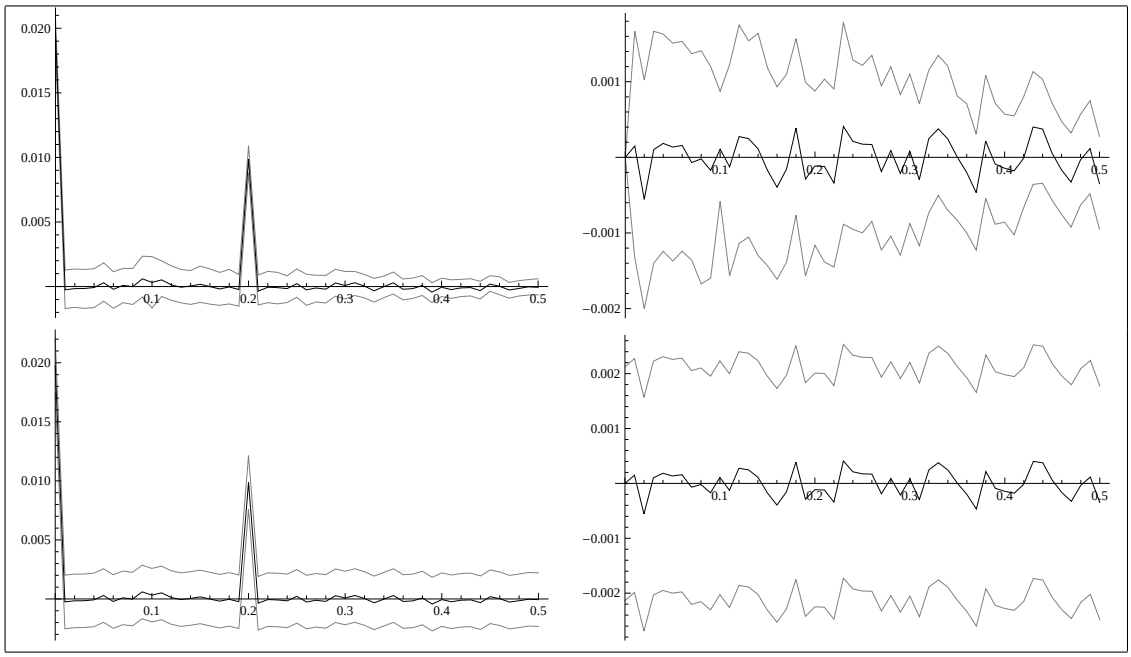

Figure 2: Results for uniform distribution. Grey color: Pointwise (first row) and simultaneous (second row) confidence intervals for $Re\,(a(\lambda,0))$ (left column) and $Im\,(a(\lambda,0))$ (right column), $\lambda \in \{0Hz, 0.01Hz, \ldots, 0.5Hz\}$ and $b = 20$. Black color: estimators of $Re\,(a(\lambda,0))$ and $Im\,(a(\lambda,0))$. Nominal coverage probability is 95%.

models have been presented in the literature in [23], [20] and [3]. These models more or less translate the reality of the measured signals. The signal may be summarized as follows: the vibration, called the meshing signal, is periodic and its frequency (meshing frequency) is equal to the frequency of rotation of one of the two wheels multiplied by the number of teeth of this wheel; Moreover, this meshing signal is modulated in amplitude and frequency by both a periodic signal of period equal to the period of rotation of the pinion and a periodic signal of period equal to the period of rotation of the wheel. In general, the frequency modulation is much less important than the amplitude modulation.

By neglecting the frequency modulations, the model established by Capdessus and Sidahmed in [4] can be used:

$$s_c(t) = \sum_{n=-\infty}^{\infty} s_e\left(t - n\tau_e\right)\left(1 + \sum_{m=-\infty}^{\infty} s_{p_1}(t - m\tau_{p_1}) + \sum_{p=-\infty}^{\infty} s_{p_2}(t - p\tau_{p_2})\right),$$

where τ_e is the meshing period, τ_{p_1} is the rotation period of wheel 1, τ_{p_2} is the rotation period of wheel 2, $s_e(t)$ is the vibratory meshing signal, $s_{p_1}(t)$ is the vibratory signal produced by wheel 1 and $s_{p_2}(t)$ is the vibratory signal produced by wheel 2.

The most striking characteristic of the signal is the amplitude modulation due to the rotation of the wheels. The spectrum will be composed by a family of lines of frequency $kf_e = k/T_e$ due to the fundamental frequency and harmonics of the meshing signal (Figure 6). This line family is spread over a large part of the spectrum, because the nature of the meshing signal is of broadband type. Moreover, the amplitude modulation results in the presence of lateral bands around the meshing harmonics, at multiple distances of $f_1 = 1/T_{p_1}$ for the modulation due to the wheel 1, and $f_2 = 1/T_{p_2}$ for the modulation due to the wheel 2.

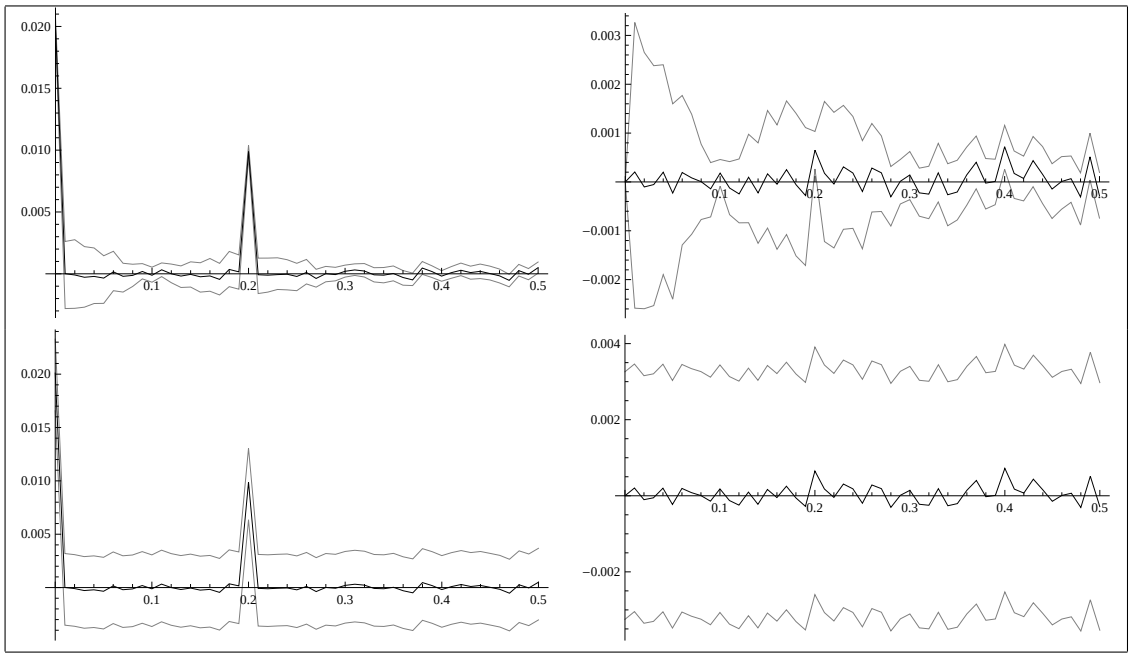

Figure 3: Results for truncated normal distribution. Grey color: Pointwise (first row) and simultaneous (second row) confidence intervals for $Re\,(a(\lambda,0))$ (left column) and $Im\,(a(\lambda,0))$ (right column), $\lambda \in \{0Hz, 0.01Hz, \ldots, 0.5Hz\}$ and $b = 100$. Black color: estimators of $Re\,(a(\lambda,0))$ and $Im\,(a(\lambda,0))$. Nominal coverage probability is 95%.

The detection and localization of the teeth defects of the wheels go through the statistical estimation of the characteristic frequencies. In the next paragraph, we will estimate the frequency of meshing a vibratory signal from a gear system.

6.2 Real vibratory signal

In this section we apply our bootstrap technique to a vibratory signal acquired with a random sampling frequency. The recordings were carried out at CETIM on a gear system with a train of gearing with a ratio of 20/21 functioning continuously until its destruction. The test was of length 12 days with a daily mechanical appraisal; measurements were collected every 24 h. These signals have already been used on several occasions to demonstrate diagnostic procedures [4] and [14]. The accelerometer signal was acquired with a sampling frequency of 20 KHz. After this signal was resampled with a uniform random temporal step. The length of the signal is 30000 and the average of this frequency is 10kHz. In this signal we have characteristic frequencies at 340 Hz and its harmonics. Additionally, for the sake of simplicity we divided observed values of the signal by 1000.
To detect significant frequencies we constructed 95% bootstrap pointwise and simultaneous confidence intervals (see Section 3.1) for $Re\,(a(\lambda,0))$ and $Im\,(a(\lambda,0))$, $\lambda \in \{300Hz, 310Hz, \ldots, 700Hz\}$, using the circular version of our bootstrap approach (see Section 4). As in Section 5 we used two block lengths $b \in \{30, 200\}$, which are approximately equal to $\sqrt[3]{n}$ and $\sqrt{n}$. The number of bootstrap samples $B = 500$. The results are presented in Figures 7-8.
Independently on the chosen block length b and used type of confidence intervals we always successfully detected frequency $340Hz$ and its harmonic $680Hz$.

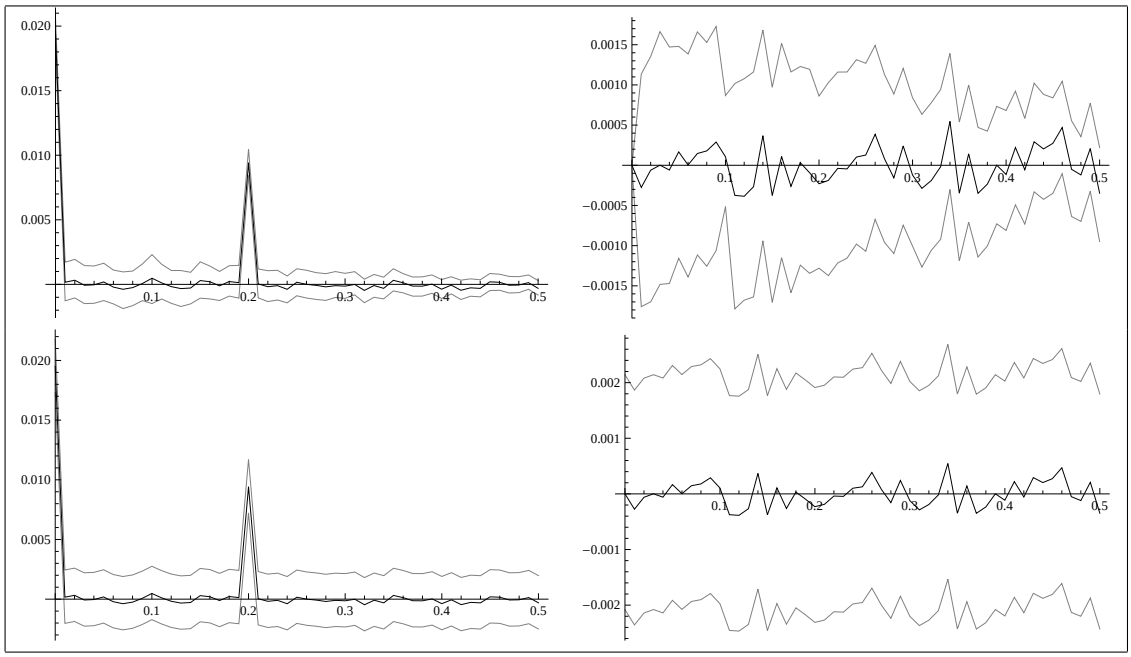

Figure 4: Results for truncated normal distribution. Grey color: Pointwise (first row) and simultaneous (second row) confidence intervals for $Re\left(a(\lambda,0)\right)$ (left column) and $Im\left(a(\lambda,0)\right)$ (right column), $\lambda \in \{0Hz, 0.01Hz, \ldots, 0.5Hz\}$ and $b = 20$. Black color: estimators of $Re\left(a(\lambda,0)\right)$ and $Im\left(a(\lambda,0)\right)$. Nominal coverage probability is 95%.

7 Appendix

For the sake of simplicity and clarity we assume that the sample size n is an integer multiple of the block length b ($n = lb$). Moreover, since the proofs for standard and circular bootstrap approaches follow exactly the same steps, we present details only for the circular method.

Proof of Theorems 4.1 and 4.2

Proof:
We need to show that the circular bootstrap method is consistent, i.e. that

$$\rho\Big(\mathcal{L}\left(\sqrt{nh}\left(\widetilde{a}(\lambda,\tau) - a(\lambda,\tau)\right)\right), \mathcal{L}^*\left(\sqrt{nh}\left(\widetilde{a}^*(\lambda,\tau) - \widetilde{a}(\lambda,\tau)\right)\right)\Big) \xrightarrow{p} 0,$$

as $n \to \infty$. At first we prove the theorem for $\Re(\widetilde{a}^*(\lambda,\tau))$. Since $\widetilde{a}^*(\lambda,\tau)$ is unbiased (see Section 4), we have that

$$\mathrm{E}^*\left(\Re\widetilde{a}^*(\lambda,\tau)\right) = \Re\widetilde{a}(\lambda,\tau).$$

By $\widetilde{\widetilde{Z}}_{t,b}$ we denote

$$\widetilde{\widetilde{Z}}_{t,b} = \sum_{s=1}^{b} \ddot{b}_{(j-1)b+s}(\tau)\cos(\lambda((j-1)b+s)h).$$

Using new notation we can rewrite the estimator $\widetilde{a}(\lambda,\tau)$ as follows

$$\widetilde{a}(\lambda,\tau) = \frac{1}{n}\sum_{j=1}^{l} \widetilde{\widetilde{Z}}_{j,b}.$$

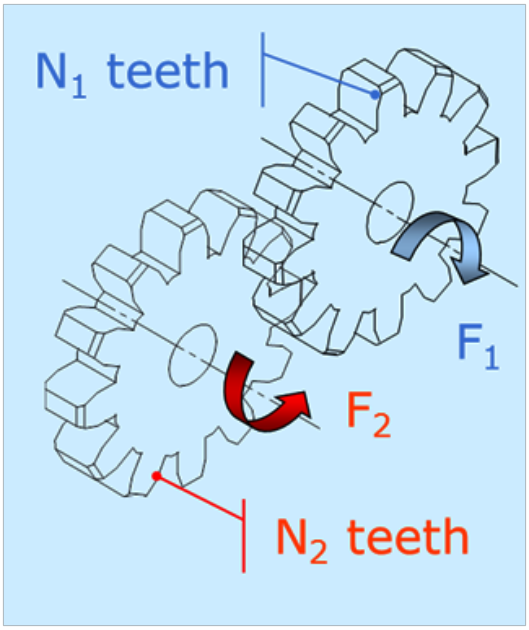

Figure 5: Single stage gear.

Correspondingly

$$\widetilde{a}^*(\lambda,\tau) = \frac{1}{n}\sum_{j=1}^{l} \widetilde{Z}^*_{j,b},$$

where

$$\widetilde{Z}^*_{t,b} = \sum_{s=1}^{b} \ddot{b}^*_{(j-1)b+s}(\tau)\cos(\lambda((j-1)b+s)^* h),$$

Additionally, let

$$Z_{t,b} = \widetilde{Z}_{t,b} - \mathrm{E}\left(\widetilde{Z}_{t,b}\right)$$

and its bootstrap version

$$Z^*_{t,b} = \widetilde{Z}^*_{t,b} - \mathrm{E}^*\left(\widetilde{Z}^*_{t,b}\right).$$

To show consistency we use Corollary 2.4.8 in Araujo and Giné(1980). We need to show that for any $\nu > 0$

$$\sum_{k=0}^{l-1} P^*\left(\frac{1}{\sqrt{nh}}\left|Z^*_{1+kb,b}\right| > \nu\right) \xrightarrow{P} 0, \tag{3}$$

$$\sum_{k=0}^{l-1} \mathrm{E}^*\left(\frac{1}{\sqrt{nh}} Z^*_{1+kb,b}\mathbf{1}_{\{|Z^*_{1+kb,b}|>\sqrt{nh}\nu\}}\right) \xrightarrow{P} 0, \tag{4}$$

$$\sum_{k=0}^{l-1} \mathrm{Var}^*\left(\frac{1}{\sqrt{nh}} Z^*_{1+kb,b}\mathbf{1}_{\{|Z^*_{1+kb,b}|\leq\sqrt{nh}\nu\}}\right) \xrightarrow{P} \sigma_1^2. \tag{5}$$

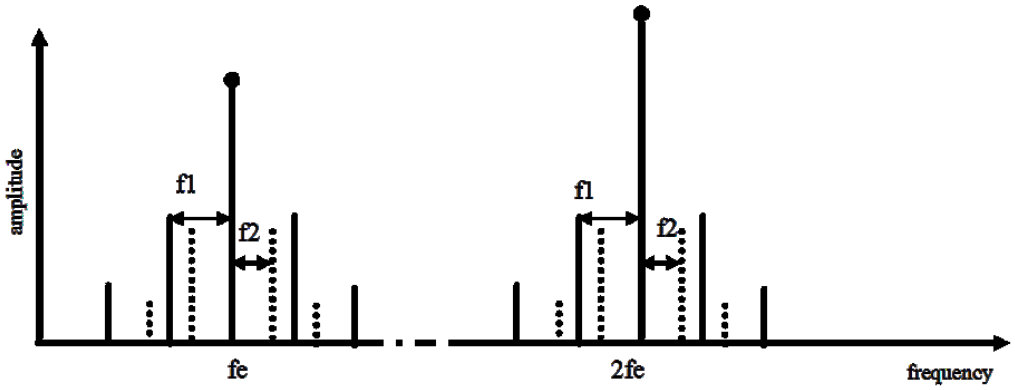

Figure 6: Gear spectrum.

Since the main steps of the proof are the same as the proof of Theorem 2 in [9], we skip technical details. The same reasoning can be applied for the imaginary case. Finally, the consistency of $\widetilde{a}^*(\lambda, \tau)$, which is the two-dimensional vector, is a consequence of the Cramér-Wold device. The same argument is used to prove Theorem 4.2.

□

References

[1] A. Araujo, E. Giné, The Central Limit Theorem for Real and Banach Valued Random Variables, Wiley, New York, 1980.

[2] A.S. Besicovitch, Almost Periodic Functions, University Press, Cambridge, 1932.

[3] C. Capdessus, Aide au diagnostic des machines tournantes par traitement de signal, PH.D dissertation, Institut National Polytechnique de Grenoble, France, 1992.

[4] C. Capdessus, M. Sidahmed, Analyse des vibrations d'un engrenage: cepstre, corrélation spectre, Traitement du Signal 8(5) (1992) 365-372.

[5] D. Dehay, Asymptotic behavior of estimators of cyclic functional parameters for some nonstationary processes, Statist. Decisions 13 (1995) 273–286.

[6] D. Dehay, A.E. Dudek, Bootstrap method for Poisson sampling almost periodic process, J. Time Ser. Anal., 36(3) (2015) 327-351.

[7] D. Dehay, V. Monsan, Discrete periodic sampling with jitter and almost periodically correlated processes, Statistical Inference for Stochastic Processes 10 (2007) 223–253.

[8] P. Doukhan, Mixing : Properties and Examples, Lecture Notes in Statistics 85, Springer, New York, 1994.

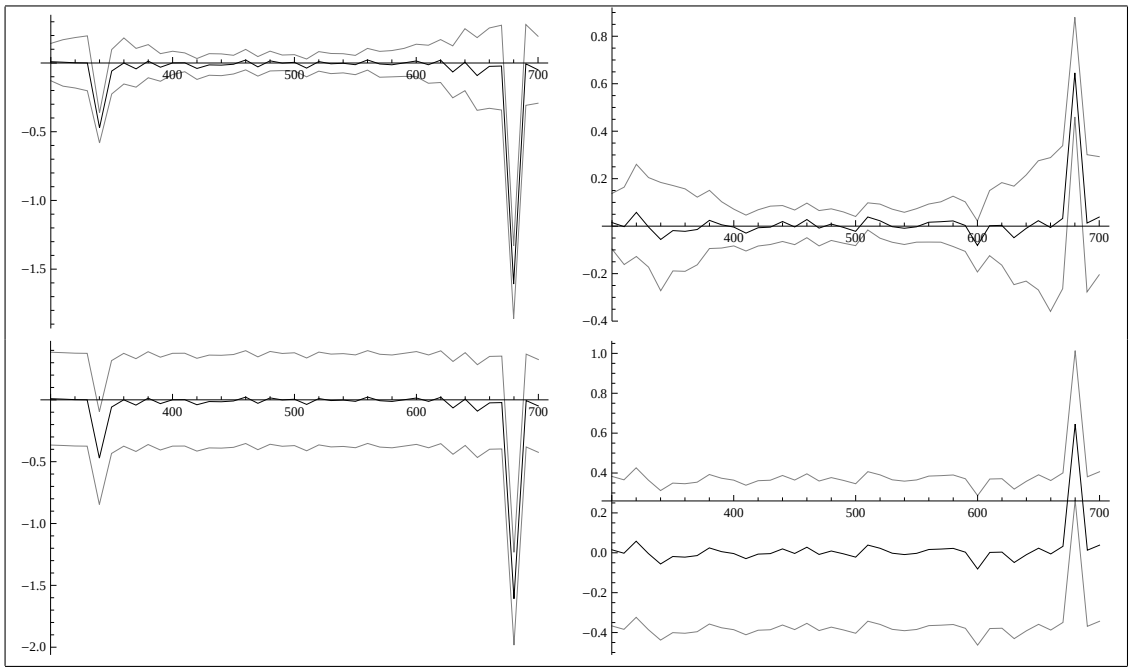

Figure 7: Grey color: Pointwise (first row) and simultaneous (second row) confidence intervals for $Re\,(a(\lambda,0))$ (left column) and $Im\,(a(\lambda,0))$ (right column), $\lambda \in \{300Hz, 310Hz, \ldots, 700Hz\}$ and $b = 200$. Black color: estimators of $Re\,(a(\lambda,0))$ and $Im\,(a(\lambda,0))$. Nominal coverage probability is 95%.

[9] A.E. Dudek, Circular block bootstrap for coefficients of autocovariance function of almost periodically correlated time series, Metrika 78(3) (2015) 313-335.

[10] A.E. Dudek, J. Leśkow, E. Paparoditis, D. Politis, A generalized block bootstrap for seasonal time series, J. Time Ser. Anal. 35 (2014a) 89-114.

[11] A.E. Dudek, S. Maiz, M. Elbadaoui, Generalized seasonal block bootstrap in frequency analysis of cyclostationary signals, Signal Process. 104C (2014b) 358-368.

[12] A.E. Dudek, E. Paparoditis, D. Politis, Generalized seasonal tapered block bootstrap, Statistics and Probability Letters, 115 (2016) 27-35.

[13] B. Efron, Bootstrap methods: another look at the jacknife, Ann Statist. 7 (1979) 1-26.

[14] M. El Badaoui, New applications of the real cesptrum to gear signals, including definition of a robust fault indicator, Mechanical systems and Signal processing 18, (2004) 1031–1046.

[15] M. El Badaoui, F. Bonnardot, Impact of the non-uniform angular sampling on mechanical signals, Mechanical Systems and Signal Processing 44 (2014) 199-210.

[16] H. Hurd, J. Leśkow, Strongly consistent and asymptotically normal estimation of the covariance for almost periodically correlated processes, Statist. Decisions 10 (1992) 201–225.

[17] H.L. Hurd, A.G. Miamee, Periodically Correlated Random Sequences: Spectral. Theory and Practice, Wiley, 2007.

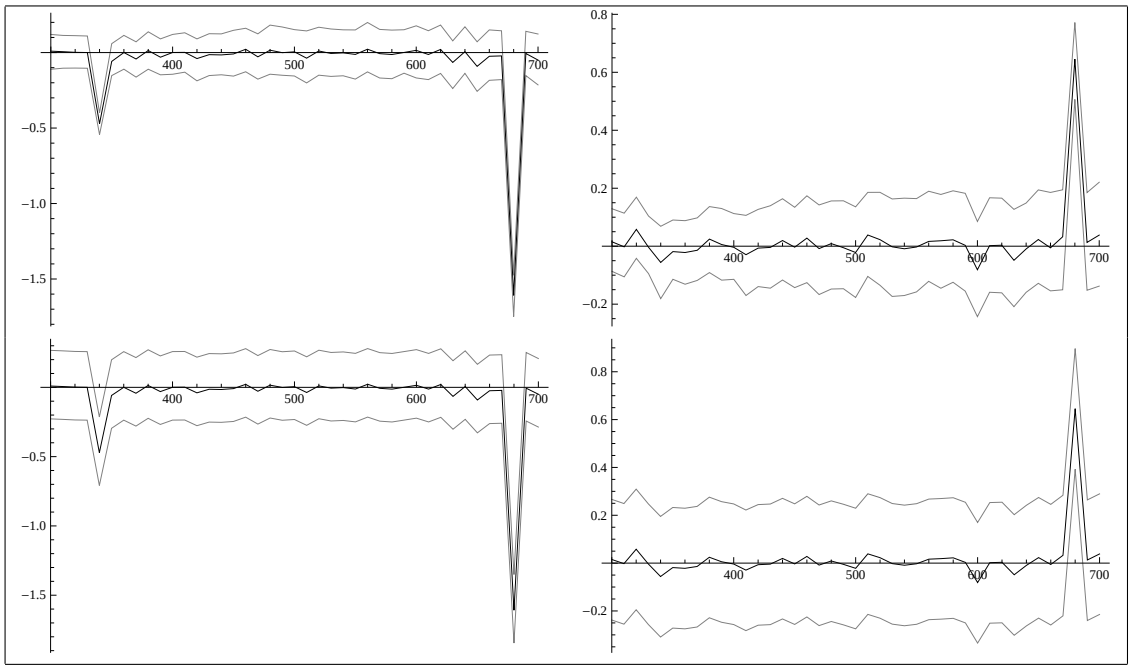

Figure 8: Grey color: Pointwise (first row) and simultaneous (second row) confidence intervals for $Re\,(a(\lambda,0))$ (left column) and $Im\,(a(\lambda,0))$ (right column), $\lambda \in \{300Hz, 310Hz, \ldots, 700Hz\}$ and $b = 30$. Black color: estimators of $Re\,(a(\lambda,0))$ and $Im\,(a(\lambda,0))$. Nominal coverage probability is 95%.

[18] H. Künsch, The jackknife and the bootstrap for general stationary observations, Ann. Statist. 17 (1989) 1217-1241.

[19] R. Liu, K. Singh, Moving block jackknife and bootstrap capture weak dependence. Exploring the Limits of Bootstrap, Wiley Ser. Probab. Math. Statist. Probab. Math. Statist. Wiley, New York, pp 225–248, 1992.

[20] P.D. McFadden, Detecting fatigue cracks in gears by amplitude and phase demodulation of the meshing vibration, J. Vib. Acoust. Stress Reliab. Des. 108(2) (1986) 165-170.

[21] A. Napolitano, Generalizations of Cyclostationary Signal Processing: Spectral Analysis and Applications, Wiley-IEEE Press, 2012.

[22] D.N. Politis, J.P. Romano, A circular block-resampling procedure for stationary data, Exploring the Limits of Bootstrap, Wiley Ser. Probab. Math. Statist. Probab. Math. Statist. Wiley, New York, pp 263-270, 1992.

[23] R.B. Randall, A new method of modelling gear faults, Journal of Mechanical Design 104 (1982) 259-267.

[24] R. Synowiecki, Consistency and application of moving block bootstrap for nonstationary time series with periodic and almost periodic structure, Bernoulli 13(4) (2007) 1151-1178.

[25] R. Synowiecki, Metody resamplingowe w dziedzinie czasu dla niestacjonarnych szeregów czasowych o strukturze okresowej i prawie okresowej, Dissertation, AGH University of Science and Techniology, Krakow, Poland, http://winntbg.bg.agh.edu.pl/rozprawy2/10012/full10012.pdf, 2008.

Acknowledgements

The authors gratefully acknowledge the support of CETIM (Centre des Etudes Techniques des Industries Mécaniques de Senlis), which provided the experimental results. Anna Dudek has received funding from the European Union's Horizon 2020 research and innovation programme under the Marie Skłodowska-Curie Grant Agreement No. 655394.